VYSOKÉ UČENÍ TECHNICKÉ V BRNĚ
Fakulta strojního inženýrství
Ústav fyzikálního inženýrství

AV ČR
Ústav přístrojové techniky

Zdeněk Pilát

OPTICKÉ MIKROMANIPULAČNÍ TECHNIKY KOMBINOVANÉ S MIKROSPEKTROSKOPICKÝMI METODAMI

OPTICAL MICROMANIPULATION TECHNIQUES COMBINED WITH MICROSPECTROSCOPIC METHODS

Teze disertační práce

Obor: Fyzikální a materiálové inženýrství

Školitel: Prof. RNDr. Pavel Zemánek, Ph.D.
Oponenti:

Datum obhajoby:

KLÍČOVÁ SLOVA

Ramanova mikrospektroskopie, optické chytání, mikrofluidika, jednobuněčné řasy, pulsní amplitudově modulovaná fluorescenční mikrospektroskopie

KEYWORDS

Raman microspectroscopy, optical trapping, microfluidics, microalgae, pulse amplitude modulation fluorescence microspectroscopy

Název pracoviště, na kterém je uložen rukopis disertační práce:

ISBN (80-214- doplní redakce)

ISSN (1213-4198)

TABLE OF CONTENTS

1 INTRODUCTION

Current optical micromanipulation techniques offer many unique tools and methods that enable spatial confinement and manipulation of microscopic objects, including living cells. A single tightly focused laser beam acts as optical tweezers (OT), allowing 3D manipulations [1] with a single object of sizes from tens of nanometers to tens of micrometers. Sophisticated setups were developed, employing beam deflectors to get several time-sharing beams [2] or dynamic phase masks to obtain so-called holographic optical tweezes [3]. Optical traps enable even simultaneous manipulation with several objects, non-contact and sterile separation of mixture components [4], spatial arrangement of particles and their transport, precise measurements of acting forces in the range of units of pN and other unique applications [5]. The laser wavelength needs to be chosen so that it is weakly absorbed by the specimen to prevent its thermal damage. Optical trapping has been combined with Raman microspectroscopy [6] to provide a non-invasive spatially resolved mapping of molecular composition of the studied sample. Recently, Raman microspectroscopy has been used to detect and identify microorganisms [7, 8], because Raman spectrum of individual microorganism serves as a unique fingerprint. Since the Raman spectral signatures represent the vibrations of molecular bonds, quantitative analyses of chemical mixtures are possible as well [9]. Both techniques, optical tweezers and Raman spectroscopy, are combined with microfluidic systems so that the fluid composition and velocity can be controlled [10]. It is also possible to create a diffusion interface between two different liquids, and individual microorganisms can be transported between the two liquids using optical tweezers [11]. Moreover, microorganisms can be isolated in micro-chambers, where their metabolic reactions can be followed by Raman spectroscopy. These techniques may find their use in fast, reagent-free identification and separation of microorganisms, and evaluation of their response to various environmental factors. The immense possibilities offered by the modern optical micromanipulation and micro-analytical techniques represent a wide platform for experimentation. We have concentrated our experimentation on Raman microspectroscopic analysis and active optical manipulation of microorganisms, and the implementation of both techniques in a microfluidic environment.

The subject of the presented Ph.D. thesis is a combination of optical micromanipulation and microspectroscopic methods. We used laser tweezers to transport and sort various living microorganisms, such as microalgal or yeast cells. We employed Raman microspectroscopy to analyze chemical composition of individual cells and we used the information about chemical composition to automatically select the cells of interest. We combined pulsed amplitude modulation fluorescence microspectroscopy, optical micromanipulation and other techniques to map the stress response of cells to various laser wavelengths, intensities and durations of optical trapping. We fabricated microfluidic chips of various designs

and we constructed Raman-tweezers sorter of micro-objects such as living cells on a microfluidic platform.

The presented selection as well as the full doctoral thesis is divided into sections dealing with the laser-induced stress in microorganisms, Raman spectral microanalysis, and optical manipulation and sorting. In this shortened version, I present a limited selection of the results presented in the full doctoral thesis.

Section 1 is dedicated to a short introduction (in full doctoral thesis accompanied with theoretical background of optical trapping, Raman spectroscopy and photosynthesis).

Section 2 describes various experiments conducted to gauge the influence of optical trapping by different laser wavelengths on the individual living cells of different microorganisms. The effects of laser irradiation were observed in terms of reproduction delay, increase of mortality, or changes in fluorescence parameters. These experiments were motivated by a need to assess the vulnerability of the selected organisms to different laser trapping wavelengths in various power ranges and durations. The resultant data were used to optimize the parameters of trapping and spectroscopic experiments on living cells.

Section 3 is dedicated to Raman analysis of microorganisms and individual cells. Analyses of Raman spectra were assessed using individual peaks, which were matched with the respective molecular vibrations based on the available data from literature and spectroscopic libraries, enabling relative quantification of chemical compounds in a mixture. These experiments were fuelled by a need to master the Raman signal collection from microorganisms and to learn understanding the links between Raman signal and chemical composition of the sample. The findings were directly implemented in the consequent Raman–tweezers experiments.

Section 4 discusses the approaches used for optical micromanipulation and sorting of cells. We present an innovative microfluidic setup for cell manipulation and sorting, and we give a description of construction and function of an active Raman-tweezers based optical sorter. This part of work was motivated by a need for a novel microfluidic Raman-tweezers sorting system that could analyze and sort various microorganisms according to their chemical properties. This system would find its use in various biological, biotechnological, chemical, pharmaceutical and other disciplines.

The whole work was summarized in general conclusions in section 5. The list of references is given in section 6. (Sections 7-9 supply the abstract in Czech language, CV and publication activities of the author.)

My personal contribution to the presented research was following: I have prepared and maintained the chemical and biological samples for the experiments. I was actively cooperating in the construction of the experimental optical apparatuses and performing the calibrations and settings. I have designed and tested multiple microfluidic setups for optical micromanipulation, including transport of living cells, cell manipulation and sorting. I have performed the spectroscopic measurements and optical manipulations of various objects including living cells of various organisms. I have analyzed the experimental data, and presented the results in oral and poster presentations at international conferences and I published my results in conference proceedings. I have published my results as a first author and as a coauthor in peer reviewed articles in various scientific journals. In cooperation with my colleagues, I have constructed a functional microfluidic Raman-tweezers based analytical and sorting system, which, to my knowledge, has no equivalent. This device is a registered utility model and has a patent pending.

2 OPTICAL TRAPPING OF MICROALGAE AT 735-1064 nm: PHOTODAMAGE ASSESSMENT

2.1 INTRODUCTION

Microbial cultures have been exploited by humanity for millennia [12]. The ever-increasing number of usable metabolites produced by microbes has driven the recent rapid development of microbial biotechnology [13, 14]. Optical non-contact micromanipulation offers an attractive opportunity to select, handle and sort individual microbial cells. Algae and cyanobacteria are susceptible to photoinhibition even when exposed to moderate photon flux densities [15]. Potentially, this hinders the application of optical micromanipulation. The absorption of light is increased by excitonic energy transfer from hundreds of pigment molecules to the reaction centers of two photosystems [16]. Photosystem II is particularly sensitive to photoinhibition during which overexcitation can result in production of harmful oxygen radicals, and other reactive species, that destroy the photosynthetic capacity of the cell and may lead to cell death [17]. To avoid this, optical trapping may employ wavelengths in the near infrared wavelength range beyond the red absorption edge of chlorophyll (which is part of PS II) [18]. In this experiment, we have explored the wavelength region suitable for optical trapping of living microalgae.

2.2 MATERIALS AND METHODS

The loss of Photosystem II activity was measured by pulse amplitude modulation (PAM) fluorescence spectroscopy [19, 20] as a loss of variable fluorescence yield F_v that is defined as the difference $F_m - F_0$ between the maximum fluorescence yield F_m and the constant fluorescence yield F_0, see figure 1. We measured changes in F_v/F_m resulting from optical trapping by focused laser radiation of different wavelengths. In accordance with available studies on other cells discussed above, we chose a

moderate trapping power of 25 mW with duration of the optical confinement of the microorganisms set to 30 s. In accordance with our previous investigations [21, 22, 23, 24] we chose the microalga *Trachydiscus minutus* for this study. *T. minutus* contains chlorophyll a, which is the central photosynthetic pigment of the vast majority of the other eukaryotic algae as well as all green plants. This makes *T. minutus* a good universal candidate for photodamage experiments.

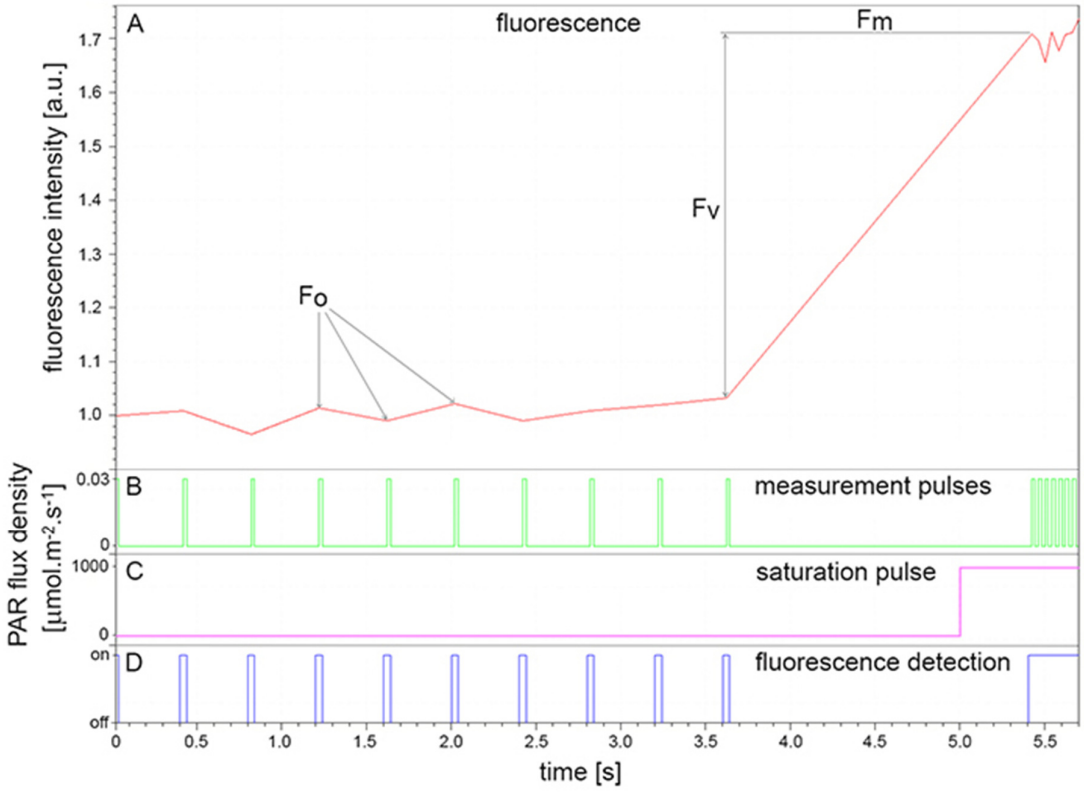

Figure 1: The diagram of PAM fluorescence measurement of F_v/F_m. A: Fluorescence intensity development in time (red line). B: Measurement pulses of white light lasting 10 µs with PAR flux density 0.03 µmol photons.m^{-2}.s^{-1} were given every 400 ms for 4 s (10 pulses) to measure the F_0 value of dark adapted algal cells (green line). C: For measurement of F_m, a saturation pulse (purple line) with PAR flux density 1000 µmol photons.m^{-2}.s^{-1} lasting 800 ms was used (time = 5s). Saturation pulse serves to reduce the primary quinone acceptor in all active Photosystem II reaction centers, therefore temporarily preventing photochemical quenching, maximizing the fluorescence. The intensity of measured fluorescence (A) was initially low (F_0), but it sharply increased after the saturation pulse was applied (F_m). Measurements of F_m and F_0 were averaged from values obtained from the individual measurement pulses. D: Fluorescence detection was switched on in periods indicated by the dark blue line. Subsequently, the variable fluorescence $F_v = F_m - F_0$ was calculated, and the F_v value was used to calculate F_v/F_m which serves as an approximation for PS II photosynthetic efficiency. Image source: FluorCam software, modified.

The experimental setup (figure 2) was based on a Micro-FluorCam system (Photon Systems Instruments, Brno, CZ). *Trachydiscus minutus* (Bourrelly) Ettl, CCALA was obtained from the Culture Collection of Autotrophic Organisms, CCALA (Institute of Botany of the ASCR, v.v.i.). The measurement of the chlorophyll fluorescence was done as described in [25], see also figure 1. FluorCam software provided measurements of F_m and F_0 fluorescence intensities. Subsequently, the variable fluorescence $F_v = F_m - F_0$, and the ratio F_v/F_m, was calculated. The first F_v/F_m value for every selected cell was recorded prior to laser trapping (time stamp: t-30). After the fluorescence measurement, the trapping laser tuned to a specified wavelength was switched on for 30 seconds. Two measurements of F_v/F_m were recorded 15 s (t+15) and 60 s (t+60) after switching off the trapping laser. Control cells were treated in exactly the same way, except the trapping laser remained off. Ten cells per treatment were used and their F_v/F_m values were averaged. The procedure was repeated for each tested laser wavelength with different cells. Measurement of the cell's response to varying trapping power (in four steps from 25 to 218 mW), was conducted at a wavelength 1064 nm (data not shown).

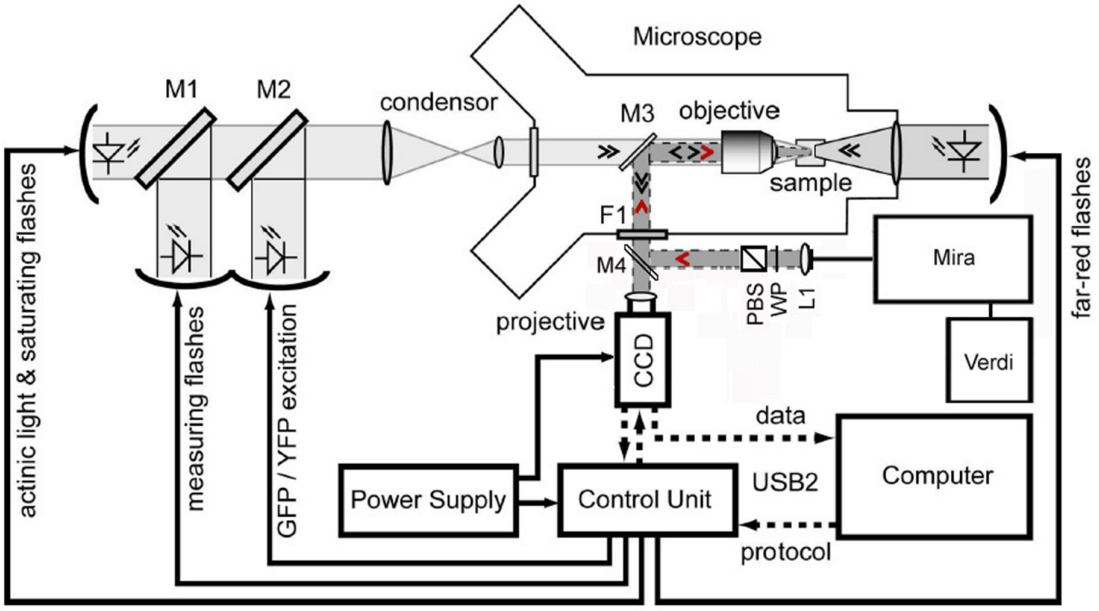

Figure 2: The experimental setup - modified Micro-FluorCam (functional scheme). LED sources and mirrors M1-M3 allow the use of various excitation sources for fluorescence (black arrows). Filter F1 blocks the LED excitation wavelengths so that they are not visible at the CCD. The trapping path (red arrows) starts at Mira emitting the trapping beam coupled to optical fiber, further collimated by lens L1 it passes through half-wave plate WP and polarizing beam splitter PBS both controlling the laser power entering the FluorCam through dichroic mirror M4 (Reproduced and modified with courtesy of Photon Systems Instruments).

2.3 RESULTS AND DISCUSSION

Figure 3 shows the F_v/F_m ratio in cells before and after 30 s of optical trapping by different laser wavelengths. Prior to trapping, the F_v/F_m ratio was between 0.3 and 0.5 which is a value significantly lower than in higher plants but typical for algae and cyanobacteria [26]. The 735 nm optical trap profoundly reduced the variable fluorescence of the trapped cells. No recovery was recorded after 15s and 60s of darkness. Only about 50% of the original F_v/F_m ratio was measured after trapping at 785 nm, and somewhat more after trapping at 835 nm. The F_v/F_m ratio before and after the trapping did not change significantly at wavelengths of 935 and 1064 nm. In a separate experiment (data not included), we shown that a trapping wavelength of 1064 nm had no damaging effect on cells with a laser power from 25 to 218 mW. F_v/F_m remained approximately the same before and after the trapping. Our finding indicates that non-invasive optical manipulation of living cells of photosynthetic microorganisms can be performed using laser wavelengths longer than 935 nm. We found that a trapping wavelength of 1064 nm caused no changes in F_v/F_m even at an incident laser power exceeding 200 mW in the sample plane. This power range is sufficient for reliable 3D manipulation of cells even in a flowing medium. Our conclusions are equally valid for other laser treatments of algal cells, e.g. laser spectroscopy.

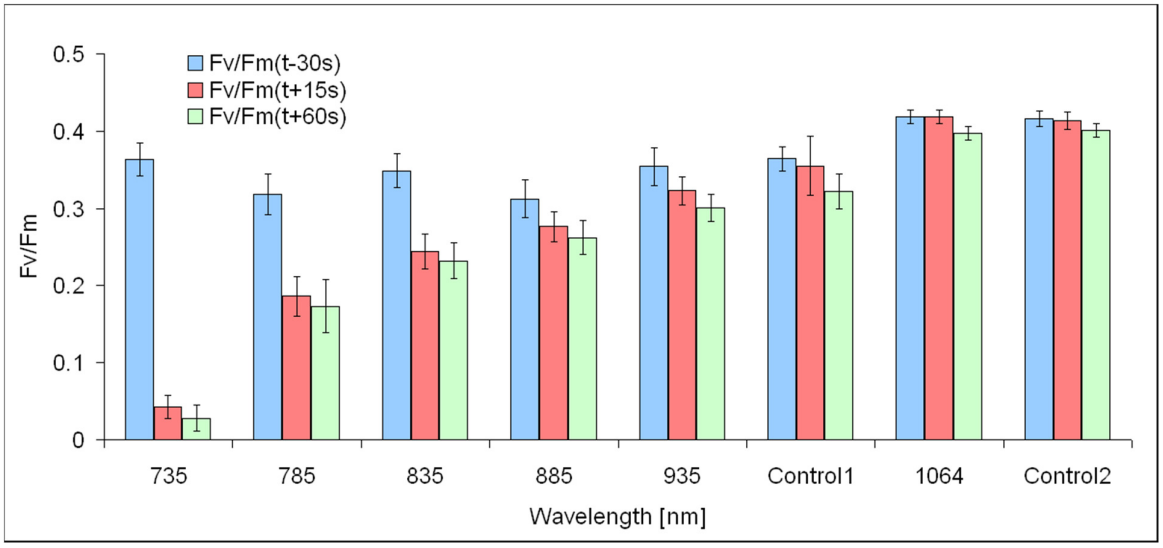

Figure 3: The Influence of the trapping laser wavelength on photosystems of *Trachydiscus minutus* cells. Trapping wavelength and control samples are defined on the horizontal axis. The quantity F_v/F_m, plotted on the vertical axis, was recorded immediately before the cell was optically trapped (t-30), 15 (t+15) and 60 seconds (t+60) after the laser was switched off (t+0) and the cell released from the trap. Ten samples were averaged for one data-point and the error-bars represent 95% confidence level.

3 RAMAN MICROSPECTROSCOPY

3.1 RAMAN MICROSPECTROSCOPY OF INDIVIDUAL ALGAL CELLS: SENSING UNSATURATION OF STORAGE LIPIDS *IN VIVO*

3.1.1 Introduction

Algae are considered as a potent source of biofuels. The most often considered product from algae for fuel industry are algal lipids [27]. In this work, we focus on the degree of fatty acid unsaturation, which is the key parameter that determines the application potential for fuels or dietary supplements or for pharmaceutical raw materials. The analysis of the fatty acid composition in algae by gas chromatography-mass spectrometry (GC-MS) has revealed a significant variability among algal species [28, 29]. GC-MS is a powerful analytic technique requiring the cell disintegration prior the analysis. Raman spectroscopy offers an attractive alternative for lipid detection that has not yet been sufficiently exploited in algae. We present Raman spectra of storage lipid bodies measured with Raman microspectroscopy in individual cells of three algal species: *Botryococcus sudeticus, Chlamydomonas* sp., and *Trachydiscus minutus*. The main driving force behind the selection of the three algal species was to estimate the applicability of the spectroscopic measurements for lipid characterization in species with significantly different relative content of unsaturated fatty acids. The intensities of the Raman spectral peaks that correspond to the saturated and unsaturated carbon-carbon bonds in lipid molecules were used to estimate the degree of unsaturation in the lipid bodies similarly to [30, 31, 32].

3.1.2 Materials and methods

Botryococcus sudeticus Lemmermann, CCALA 780 (VAZQUEZ-DUHALT/UTEX 2629), *Chlamydomonas* sp. CCALA, and *Trachydiscus minutus* (Bourrelly) Ettl, CCALA, were obtained from the Culture Collection of Autotrophic Organisms, CCALA (Institute of Botany, Academy of Sciences of the Czech Republic). For *in vivo* microspectroscopic experiments with spatially immobilized algal cells, 2-4% w/v solution of low temperature melting agarose (Sigma, Type X1) in deionized water was mixed with 10-30% v/v of algal suspension directly on a microscope cover slip. Raman microspectroscopic experiments were carried out using a home-built experimental system. The layout of this system is shown in figure 4. In order to extract quantitative information from the experimentally obtained spectral data, we adopted the rolling circle filter (RCF) technique for background removal. In our experiments, we determine the ratio of unsaturated-to-saturated carbon-carbon bonds in algal lipid molecules with two specific spectral peaks at Raman shifts ν_U = 1656 cm^{-1} (cis C=C stretching mode proportional to the amount of unsaturated C=C bonds,) and ν_S = 1445 cm^{-1} (CH_2 scissoring mode proportional to the amount of saturated C-C bonds).

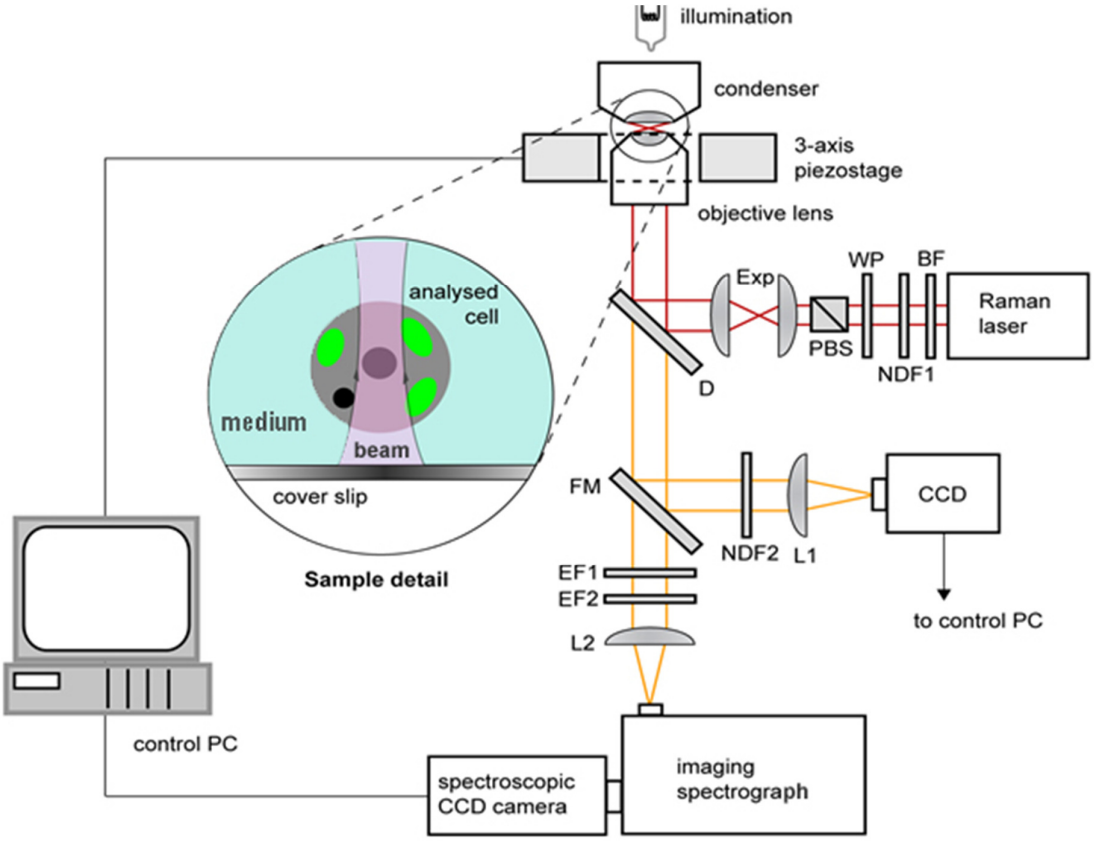

Figure 4: Schematic diagram of the experimental setup for Raman microspectroscopy. BF – bandpass filter, D – dichroic mirror, Exp – beam expander, FM – flipping mirror, L1,2 – lenses, NDF1,2 – neutral density filters, EF1,2 – edge filters, PBS – polarizing beam splitter, WP – lambda-half wave plate. Inset shows the detail of the studied sample.

3.1.3 Results and discussion

As expected, the obtained values of $I_R(\nu_U)/I_R(\nu_S)$ are directly proportional to the calculated values of $N_{C=C}/N_{CH2}$ (figure 5) for individual fatty acids because $I_R(\nu_U)$ (respectively $I_R(\nu_S)$) scale linearly with the numbers $N_{C=C}$ (respectively N_{CH2}) of C=C (respectively CH_2) groups per molecule.

Figure 6 shows typical Raman scattering spectra obtained from intracellular lipid bodies in the three studied algal species. It is clearly visible that the ratios $I_R(\nu_U)/I_R(\nu_S)$ of the Raman spectral peaks at 1656 cm^{-1} and 1445 cm^{-1} differ for individual species; specifically *Trachydiscus minutus* has a significantly higher content of the unsaturated fatty acids in comparison with the other two species. We calculated the average mass unsaturation ratio $N_{C=C}/N_{CH2}$ for the selected algal

species and verified the data obtained from Raman microspectroscopic measurements by comparing them with GC-MS analysis of the algal fatty acid composition. As mentioned above, GC-MS is a well-established technique that provides a robust benchmark for our results. From the GC-MS results, we also determined the average mass unsaturation ratio $N_{C=C}/N_{CH2}$. We found an excellent agreement between the two methods of unsaturation determination. Hence, we conclude that the *in vivo* obtained Raman spectroscopic data can indeed serve as a robust and reliable indicator of the unsaturation of algal storage lipids.

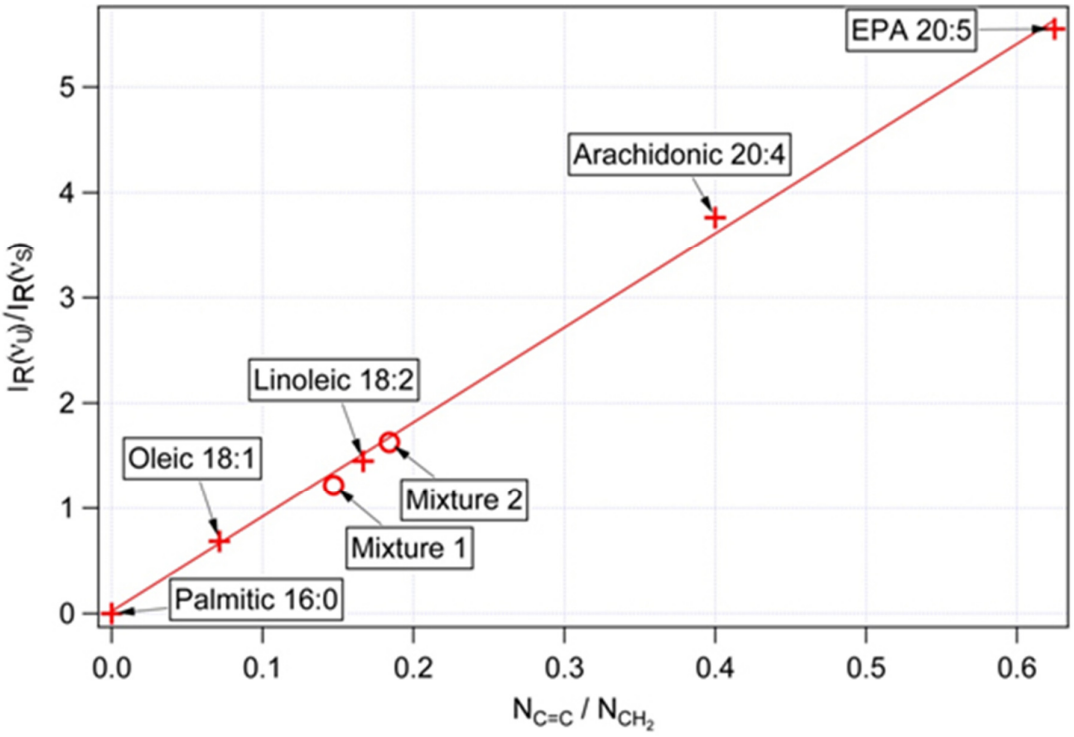

Figure 5: Dependence of the observed Raman intensity ratio $I_R(\nu_U)/I_R(\nu_S)$ on the molecule mass unsaturation $N_{C=C}/N_{CH2}$. Crosses mark experimental data obtained with pure fatty acids, straight line is a fit of this data. Circles indicate verification data points obtained with mixtures of oleic and arachidonic acids of different molar ratios; this data was not included in the fit.

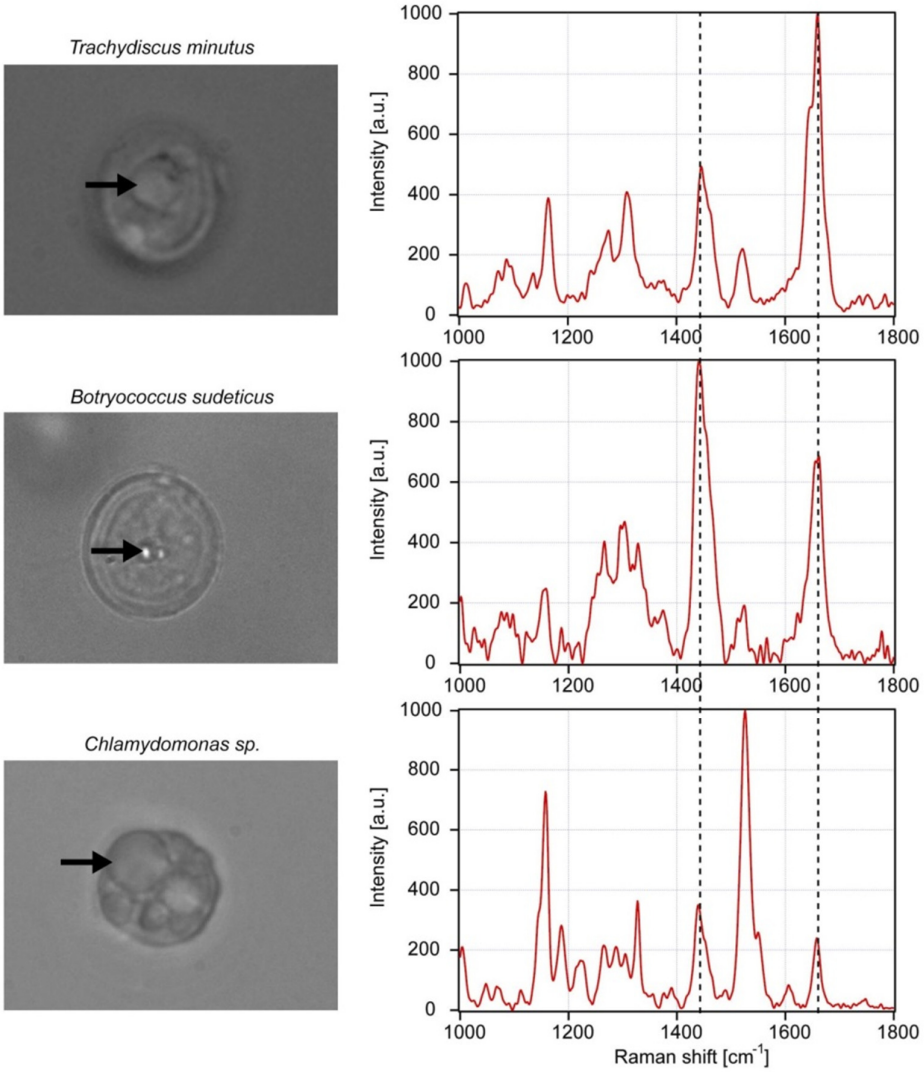

Figure 6: Typical Raman scattering spectra of intracellular lipid bodies contained in three different algal species: *Trachydiscus minutus* (top), *Botryoccocus sudeticus* (middle), and *Chlamydomonas* sp. (bottom). Raman bands used for the calculations of iodine value are highlighted with dashed vertical lines. Corresponding pictures to the left of the spectra show the lipid bodies from which the spectra were recorded (indicated by the black arrows).

3.2 RAMAN MICROSPECTROSCOPY OF ALGAL LIPID BODIES: MEASURING B-CAROTENE CONCENTRATION

3.2.1 Introduction

The aim of this experiment was to achieve direct measurement of β-carotene concentration in algal lipid bodies by Raman microspectroscopy. Algae were cultivated in a light intensity gradient to induce a gradual increase of β-carotene and storage lipid production. We used algal suspension embedded in agarose gel. Raman

spectra were recorded along with bright-field (BF) microscopic images. We have employed a calibration set of β-carotene solutions in a vegetable oil for absolute reference. From the obtained calibration curve, we have calculated the absolute concentrations of β-carotene in the lipid bodies (LBs) of the sampled algae. Furthermore, we have compared the β-carotene-to-lipid Raman peak ratio with the light intensity during the cultivation and the LB volume calculated from the BF image analysis.

3.2.2 Materials and methods

Raman microspectroscopic experiments with living algal cells were carried out using a homebuilt experimental system. Lipid body volume (V_{LB}) was calculated based on a spherical approximation of the LB shape. In order to calibrate the measurements, pure β-carotene (Sigma-Aldrich) was dissolved in commercial extra virgin olive oil resulting in six standard solutions containing 0.007-10.0 $g.l^{-1}$ of β-carotene, which were spectrographed with integration time 0.1 s at 150 mW laser power, wavelength 785 nm. Characteristic Raman peaks of β-carotene and lipids were selected and their magnitudes were used for calculation of various simple and combined ratios in order to obtain the best correlation with the β-carotene concentration in the oil solutions. The most suitable ratio was subsequently used for calculation of a calibration curve, and the β-carotene concentration in the algal LBs. In order to prevent miscalculations due to the minor drift of the Raman peaks, we evaluated the maximal intensity of the peak from a 20 cm^{-1} interval centered on the nominal Raman shift value.

3.2.3 Results

BF microscopy was used to examine the ultrastructural features of the studied algal cells. In this experiment, PAR flux density over 500 $\mu mol.m^{-2}.s^{-1}$ induced substantial enlargement of the lipid bodies. Selected cells of *Trachydiscus minutus* cultivated in low, medium and high illumination and the spatially resolved Raman spectra of their intracellular lipid bodies are depicted in figure 7. Intensive β-carotene Raman spectral signatures were detected, while the lipid signals were comparatively weak. In general, the Raman signal of β-carotene was increasingly dominant in cells with intensifying PAR illumination, and particularly in LBs of large volume. We have employed a set of β-carotene solutions to calibrate the Raman measurements of LBs on the absolute concentration scale, see figure 8. The ratio of Raman signals used for β-carotene quantification $I_R(\beta)$ was

$$I_R(\beta)=I_R(\nu_B)/[I_R(\nu_{CH2})+I_R(\nu_{C=C})]. \qquad \textit{Equation 3.2.3.1}$$

The correlation of this Raman ratio with β-carotene concentration reached coefficient of determination $R^2 = 0.9961$. The calibration equation

$$I_R(\beta) = 2.8175\ c_\beta + 0.462 \qquad \textit{Equation 3.2.3.2}$$

was derived from a linear fit and it was used to calculate the absolute β-carotene concentrations in the examined lipid bodies. The incorporation of both saturated and unsaturated lipid indicators may improve the measurement reliability in variably saturated lipid mixtures.

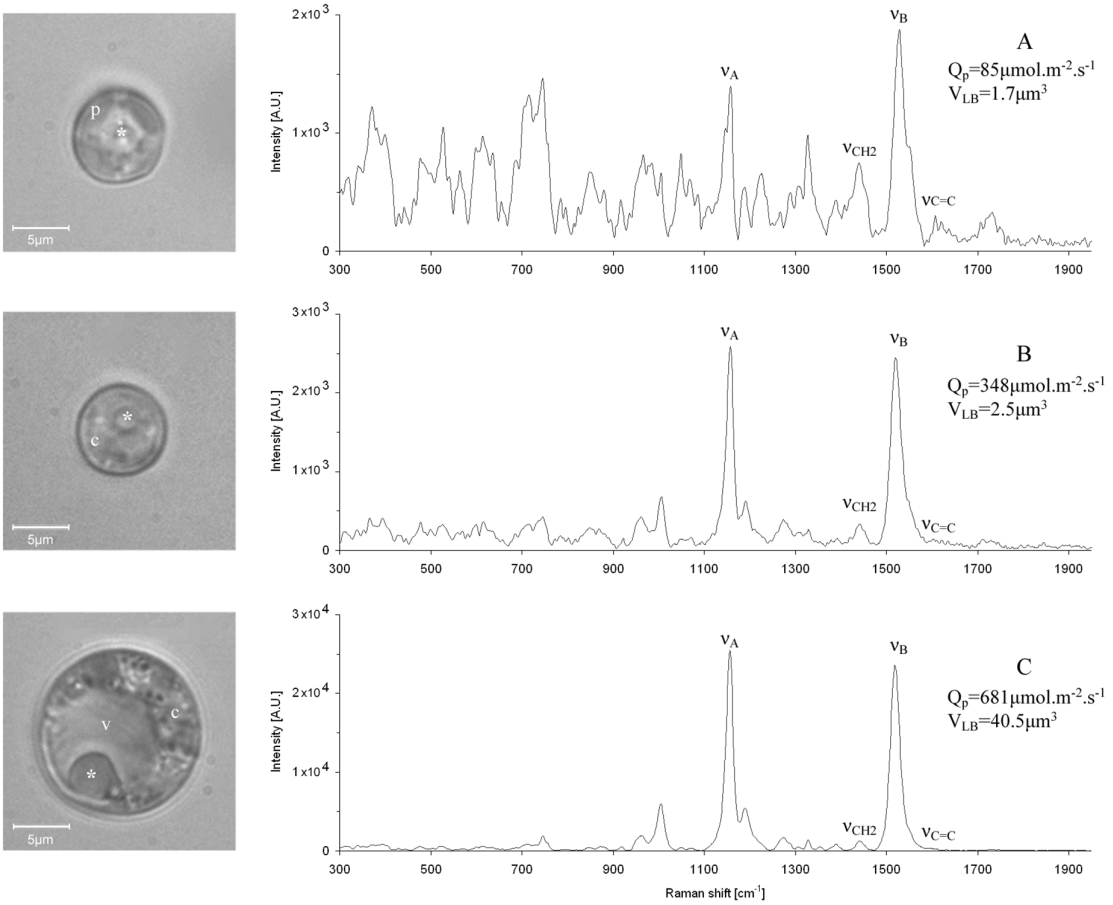

Figure 7: Raman spectra of *Trachydiscus minutus* lipid bodies. The images on the left side show the spectrographed cells. Lipid bodies targeted by the Raman laser are indicated by the white asterisks (*). Lipid body volume V_{LB} increased with PAR intensity Q_p. Oval chromatophores (pp), well-formed and uniformly distributed in low PAR illumination, became gradually more miss-shaped, reduced in number and restricted to a smaller area of cytoplasm (c), exposing the translucent vacuole (v) with increasing PAR intensity. Raman spectra of the respective LBs on the right side show the increasing magnitude I_R of β-carotene peaks at 1157 cm^{-1} (ν_A) and 1525 cm^{-1} (ν_B), while the spectral features of other cellular components including lipids at 1445 cm^{-1} (ν_{CH2}) and 1656 cm^{-1} ($\nu_{C=C}$) present comparatively small changes in their absolute magnitude. The $I_R(\nu_A)/I_R(\nu_B)$ ratio changes considerably with the LB volume and cultivation conditions.

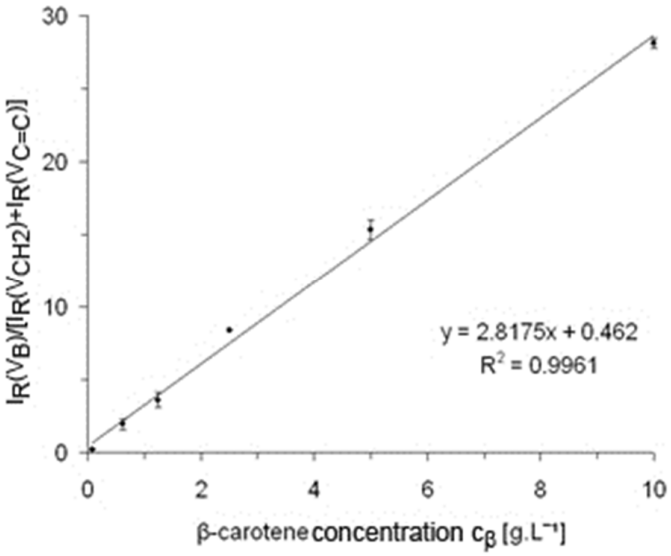

Figure 8: Calibration of Raman signal ratio with β-carotene solutions. β-carotene solutions were spectrographed and the calculated ratios $I_R(\beta)=I_R(\nu_B)/[I_R(\nu_{CH2})+I_R(\nu_{C=C})]$ were correlated with the known β-carotene concentrations c_β, yielding the coefficient of determination R^2 = 0.9961. The absolute concentration of β-carotene was calculated from the Raman signal ratio $I_R(\beta)$ using linear regression to obtain the *equation 3.2.3.2*. Error-bars: 2 standard deviations.

The maximal detected β-carotene concentration in the storage lipids of *T. minutus* was around 8 $g.l^{-1}$. We correlated the calculated β-carotene concentrations in individual LBs to their respective volumes (V_{LB}), see figure 9. In general, the experimental cultures displayed light stimulated LB volume enlargement in direct proportion with the increasing β-carotene concentration c_β. The variability between the individual specimens was high, considerable proportion of the examined cells was showing either relative overproduction or underproduction of β-carotene per LB volume. The β-carotene concentration c_β and lipid body volume V_{LB} were found to be proportional in certain extent to the PAR intensity, see figure 10. PAR intensity over 500 $\mu mol.m^{-2}.s^{-1}$ induced lipid accumulation, on average the LBs reached around 2.6 fold increase in volume compared to the low light variants. The detected concentration of β-carotene followed a similar trend, reaching in average 2.8-fold increase. The described simple Raman assisted method of β-carotene concentration estimation could find its use in the non-invasive detection of β-carotene overproducing cells. Moreover, this technique could aid fast semi-quantitative discrimination between small (e.g. $V_{LB}<10\ \mu m^3$) and large (e.g. $V_{LB}>10\ \mu m^3$) lipid bodies. Thanks to high intensity of β-carotene spectral signatures, the detection of very large or β-carotene rich lipid bodies for the purpose of Raman assisted sorting could be achieved with integration times in order of milliseconds with laser power in 100 mW range at 785 nm wavelength.

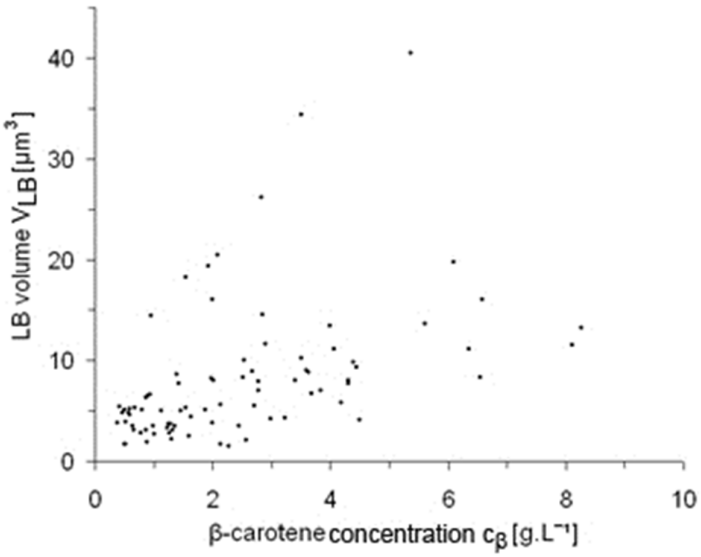

Figure 9: Proportionality of β-carotene concentration c_β and LB volume V_{LB}. The concentration of β-carotene c_β was derived from the Raman signal ratio and plotted against the volume of the lipid body V_{LB}. Cells displayed light stimulated increase of lipid body volume, which was loosely proportional with the β-carotene accumulation. The cells with abnormal quantities of β-carotene can be clearly distinguished. In total, 85 measurements were conducted.

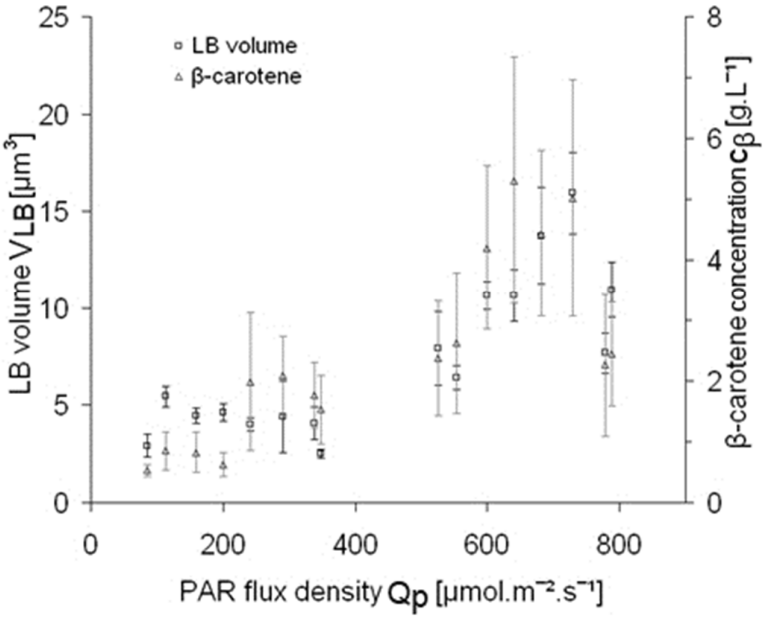

Figure 10: Proportionality of β-carotene concentration and LB volume to PAR intensity. The lipid body volume V_{LB} and the Raman-derived β-carotene concentration c_β were averaged within the 16 individual experimental variants and plotted against the PAR flux density. $Q_p > 500$ µmol.m^{-2}.s^{-1} induced intensive lipid accumulation. On average, the LBs reached around two-fold increase in volume compared to the low light variants. Error-bars: 2 standard deviations.

4 RAMAN TWEEZERS IN VERTICAL MICROFLUIDIC SYSTEM FOR ANALYSIS AND SORTING OF LIVING CELLS

4.1 INTRODUCTION

We have devised an analytical and sorting system combining optical trapping with Raman spectroscopy in microfluidic environment in order to identify and sort biological objects, such as living cells of various prokaryotic and eukaryotic organisms. Our main objective was to create a robust and universal platform for non-contact sorting of micro-objects based on their Raman spectral properties. This approach allowed us to collect information about the chemical composition of the objects, such as the presence and composition of lipids, proteins, or nucleic acids without using artificial chemical probes such as fluorescent markers. The non-destructive and non-contact nature of this optical analysis and manipulation allowed us to separate individual living cells of our interest in a sterile environment and provided the possibility to cultivate the selected cells for further experiments. Such systems could find their use in many medical, biotechnological, and biological applications. The vertical sorting setup is a micro-Raman tweezers application designed for sorting of cells that may pose problem for traditional sorting mechanisms, e.g. horizontal microfluidic channels or FACS. We used algal cells, which are strongly adhesive, tend to form clusters, and can be sized over 20 μm in diameter. The system uses a special microfluidic chip. The setup was designed to eliminate the problems of cell sedimentation and adhesion in the channels, and to simplify the means of propulsion of cells in the system by exploiting gravity. The system can provide information about the chemical nature of the studied objects, and it is equipped by a dedicated universal software for automated sorting of many different objects of interest.

4.2 MATERIALS AND METHODS

Raman tweezers experiments with living cells were carried out using a home-built experimental system, see figure 11. The optical trapping and Raman excitation was done by a single focused beam. Maximal laser power used for the excitation and trapping was 200 mW at the specimen plane. The microfluidic chip was held on a micropositioning platform (Microstage-20E, Mad City Labs) providing movement of the sample with respect to the objective lens. Electrically actuated shutter S (SH05, Thorlabs) was used to block the laser beam when necessary. We were able to safely move with the microorganisms with maximal speed of 15 μm/s.

Microfluidic channels were fabricated in polydimethylsiloxane (PDMS) using soft lithography [33]. *T. minutus* was cultivated in several batch cultures, which were taken after various periods of cultivation, up to several months. Culture A was about 3 weeks old aliquot from a constantly aerated cultivation, and it received the smallest light intensities. Culture B was about 10 weeks old and it received medium

light intensities. Culture C was about 18 weeks old and it received the highest light intensity for the longest time. While the culture A was green, the culture B was green-brownish, and the culture C was brown. An adjustable pipette with a special narrow tip (Eppendorf Microloader) was used to load the sample. The cell suspension was aspirated into the pipette tip and transferred into the chip, see figure 12.

The control software for the Raman tweezers sorting system was built in LabView. After initialization, graphical user interface (GUI) is used for setting the parameters of the system. The object recognition module detects the cells in the ROI and moves the stage horizontally, until the closest detected cell falls into the range of the optical trap. The cell is trapped and the Raman spectrum is recorded. The spectrum is then filtered and the maximal intensities in selected Raman shift areas are calculated (for example 1440 cm^{-1} and 1660 cm^{-1} for calculation of lipid unsaturation [53]). The ratio of these two numbers is then displayed in a dedicated table along with the number of the sampled cell. Concurrently, an image of the analyzed cell is taken and the whole Raman spectrum is saved in a form of a text file. The table of the Raman spectral ratios continually calculates the mean value from all the samples. The operator can then use this value to regulate the stringency of the cell selection, by choosing the right value of the critical ratio, above which the cells will be selected. After setting this ratio to the correct value, the software continues the sorting as long as there are cells to trap. It is obvious that selected method does not sort all the cells in the sample, nevertheless, the sample can be passed through the system several times.

When the system collected the cells of desired properties, all the liquid in the vertical channel was aspirated into the syringe until the vertical channel was empty. The chip was cautiously removed from the holder without disturbing the pipette tip blocking the port of the side channel. The chip was then incubated in upright position for approximately 6-12 hours in room temperature and high humidity (>90%) to allow the cells to sediment and attach themselves to the agarose surface. Then the pipette tip was removed from the chip. Under binocular microscope, the part of the agarose plug containing the cells was gently pushed out of the pipette tip on a microscope slide for immediate observation or on the surface of a suitable solid cultivation medium. The selected cells were then cultivated in standard conditions.

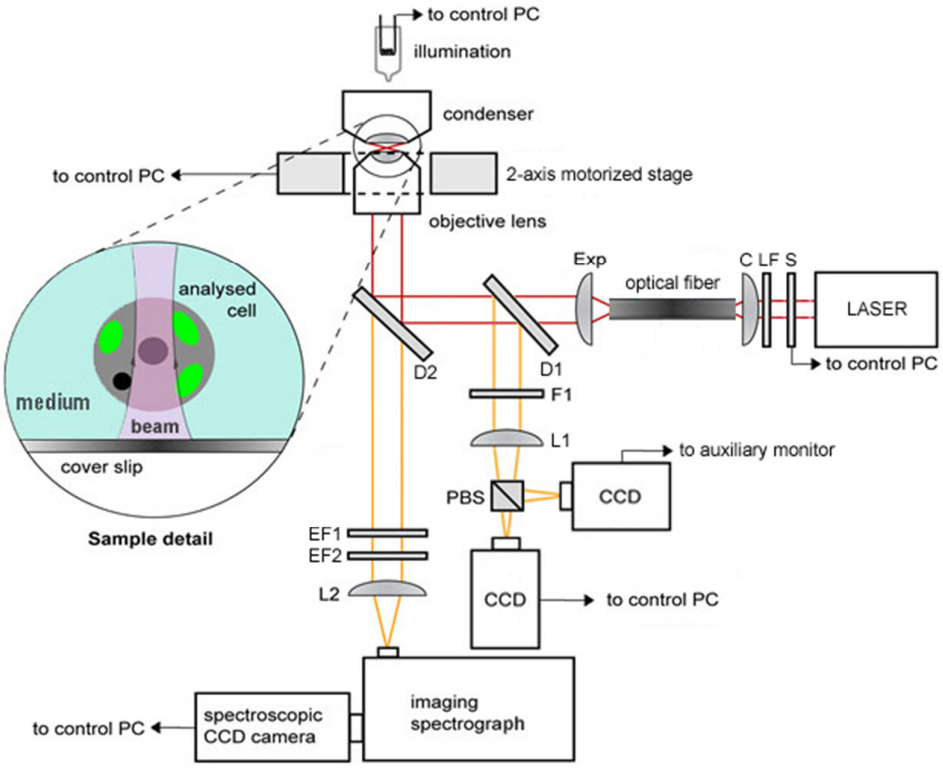

Figure 11: Schematic diagram of the vertical sorting setup combining Raman microspectroscopy with optical tweezers. Raman excitation laser serves also for trapping and it is delivered through shutter S, line filter LF and coupling lens C into an optical fiber. The beam is expanded by an expander Exp, passes dichroic mirror D1, reflects from dichroic mirror D2 and enters the objective lens. Raman signal from the specimen passes D2, edge filters EF1,2 and is focused by lens L2 into the spectrograph. Illumination light reflects from both D1 and D2 and is coupled to two CCD cameras via filter F1, focusing lens L1 and beam-splitter PBS. Inset shows the detail of the studied sample.

4.3 CELL ANALYSIS AND SORTING BY RAMAN TWEEZERS IN MICROFLUIDIC CHANNEL

The effectivity of recovery of the selected cells from the chip and other basic system parameters were tested by mixing the cells of *T. minutus* with polystyrene beads (7 μm diameter). The mixture consisting of approximately equivalent concentration of polystyrene beads and algal cells was sorted to isolate the cells based on the ratio between the intensities of Raman peaks typical for polystyrene (1001 cm^{-1}) and for β-carotene in algae (1525 cm^{-1}), denoted $I_R(\nu_{1525})/I_R(\nu_{1001})$, see figure 13. The selected critical ratio was 1. 50 cells were sorted to the side channel. The system lost ~75% of objects (cells and polystyrene beads) during an attempt to optically trap, during spectral analysis or during transport in optical trap. The losses were caused mainly by inefficient trapping of objects far from the focal plane and by collisions with other cells or beads. The difference in Raman spectra between cells

and polystyrene beads was resolved with accuracy close to 100%. Unwanted exchanges of cells for beads or other cells during optical trapping after Raman analysis caused contamination ~10% in the isolated sample. In this experiment, we have isolated 38% of the selected cells from the agarose plug. The isolated cells appeared anatomically normal when inspected under microscope (BF, magnification 150X and 600X) with no obvious signs of photodamage (bleaching of chlorophyll, atypical morphology) 13 hours after the sorting.

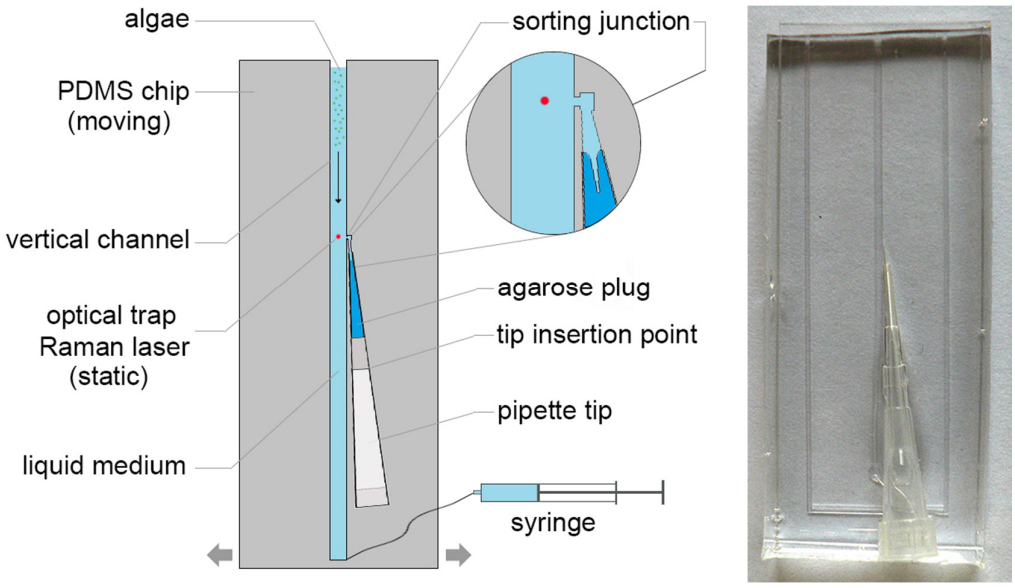

Figure 12: Schematic representation and a photograph of the microfluidic part of the Raman-tweezers sorter. Left: Scheme of the vertical sorting chip with microfluidic circuits. Biological sample (e.g. algae) is top-loaded into a vertical channel. As the cells fall through the column of liquid medium, they are recognized, optically trapped, spectrographed and moved through the sorting junction to the side-channel if it is desirable. The selected cells are collected in a conical reservoir inside an agarose plug in a pipette tip connected via the insertion point to the sorting junction, see the circular inset. The syringe serves to fill and empty the main channel. Right: Image of the microfluidic chip from PDMS bonded to a glass cover slip in oxygen plasma. Vertical channel and the ports for the microfluidic tube and for the pipette tip are visible; the tip is inserted in the port.

The sorting speed was strongly varying in time. It reached up to about one object (cell or bead) every 10 seconds, equivalent to 360 objects per hour, when about 50% of the trapped objects were transported to the side channel and when the optical trapping was successful in 100% cases during the time of observation. The sorting speed was considerably higher when the proportion of selected cells was low, e.g. 0.1%. Depending on the density of the suspension, it occasionally reached up to one object every 5 seconds (~720 objects per hour). However, the average sorting speed

over longer period was considerably lower, due to fluctuations in cell suspension density around the sorting area. The effective sorting speed was defined as a number of objects the system attempted to sort during 2 hour interval minus the objects lost from optical trap and exchanged cells, while 50% of the trapped objects were transported to the side channel. The effective sorting speed was estimated to be ~90 objects per hour.

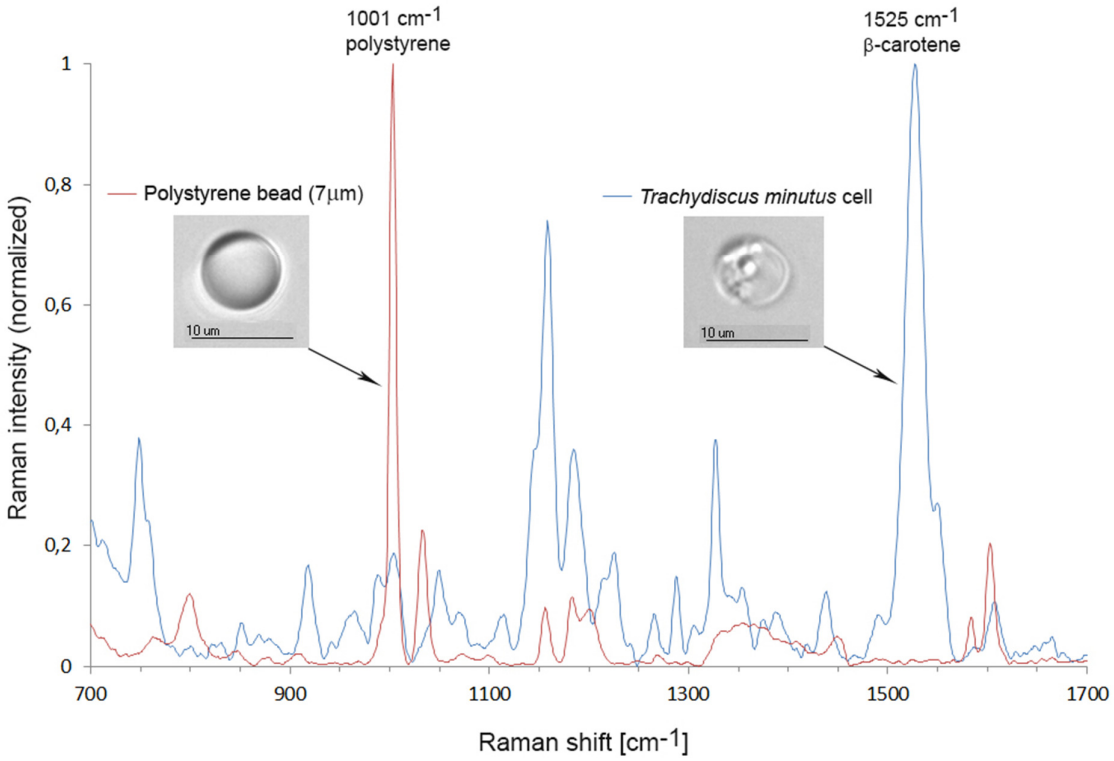

Figure 13: Raman spectra of optically trapped polystyrene bead and a cell of *T. minutus*. The polystyrene ring breathing vibration at 1001 cm^{-1} and β-carotene double bonds vibration at 1525 cm^{-1} that were used for particle sorting are denoted by their Raman shifts and by images of the respective particles.

We have tested the sorting system with different populations of alga *T. minutus*. First, the cells were sorted arbitrarily to test the ability of the system to move the selected cells to the desired location in the horizontal channel. See figure 14. Then, based on the average ratio between the intensities of the Raman peaks (1440 cm^{-1} and 1660 cm^{-1}), the critical ratio was selected and the system was allowed to sort cells in a fully automatic regime. During the sorting process, the Raman spectrum and the image of the sorted cell were collected. The examples of the typical object images taken after the Raman spectra acquisition are in figure 13.

The ratio of the intensity maxima at 1660 cm^{-1} and 1440 cm^{-1}, denoted $I_R(\nu_U)/I_R(\nu_S)$ was calculated from the obtained Raman spectra for each sampled cell

and plotted against the sample number to visualize the variability within and between the experimental populations A, B, and C, of *T. minutus*. The average values and standard errors were calculated to demonstrate the statistical difference in the lipid unsaturation defining ratio $I_R(\nu_U)/I_R(\nu_S)$, see figure 15. We found that the population A, that received the shortest period of nutrient stress and only mild light intensities during the cultivation, possessed the highest $I_R(\nu_U)/I_R(\nu_S)$ ratio which was interpreted as a relatively high level of cellular lipids unsaturation. This is about 0.1 in terms of mass unsaturation $N_{C=C}/N_{CH2}$, equivalent to a mixture of oleic (18:1) and linoleic (18:2) acid. The longer periods of nutrient stress and higher light intensity during cultivation in populations B and C have caused gradual reduction of the $I_R(\nu_U)/I_R(\nu_S)$ ratio which translates to gradually lower production of unsaturated lipids. The lowest detected mass unsaturation $N_{C=C}/N_{CH2}$ was around 0.01, equivalent to almost purely saturated fatty acids, e.g. palmitic (16:0). The quantitative relation between $I_R(\nu_U)/I_R(\nu_S)$ and unsaturation $N_{C=C}/N_{CH2}$ is discussed in reference [21] and in section 3.1.

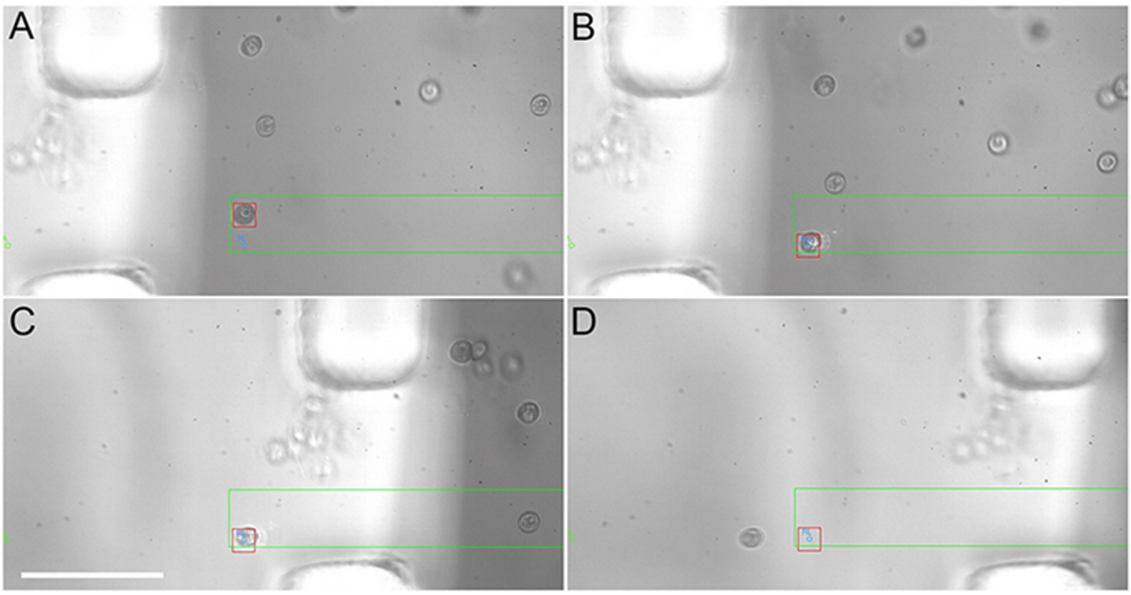

Figure 14: Sequential figures of cell sorting. Screen grab sequence from the working sorting system GUI shows the image from the CCD camera. A: A cell in the green square region of interest is recognized which is indicated with the red box around it. The optical trap is positioned below the cell. B: The cell is trapped at the laser spot, indicated by the blue circle. Illumination light is turned off, Raman spectrum is recorded, ratio of selected peaks is calculated and decision is made whether to select or refuse the analyzed cell. C: The selected cell is moved through the sorting junction to the side channel, from where it falls to the agarose target. D: The cell is released from the trap and the trap returns to the vertical channel for another cell. The position of the trap is always fixed, while the chip moves on the motorized stage. The scale bar (white) is 40 µm long.

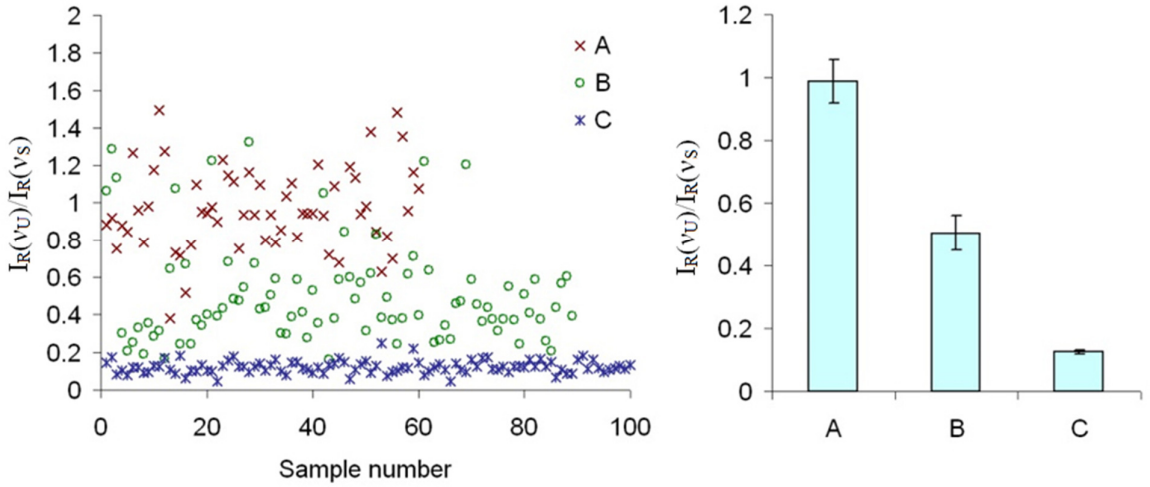

Figure 15: Left: The distribution of the Raman unsaturation parameter $I_R(\nu_U)/I_R(\nu_S)$ in the selected populations of *T. minutus*. Right: The average unsaturation $I_R(\nu_U)/I_R(\nu_S)$ of the selected populations of *T. minutus*. Error-bars represent the 95% confidence level. Number of used samples: A: 60, B: 89, C: 134.

4.4 DISCUSSION

The use of the traditional horizontal microfluidic setups is limited by the intensive tendency of large algal cells to settle at the bottom of the channel. This in turn provokes creation of cell lumps that cause trapping and sensing problems. We have tested an alternative approach with a vertical microfluidic channel where the contact of the cells with the wall is eliminated and the cells were propelled in the channel by the gravity force. This PDMS channel was integrated into an optical setup providing automated optical trapping of the falling cells and acquisition of Raman spectra from a single trapped cell of sizes from few micrometers up to several tens of micrometers. Real time analysis of the Raman spectra signatures allows sorting of living cells according to character of the chemical bonds present in the biological structures inside the cell. We proved that our sorting system is capable of automatic object recognition, optical trapping, Raman spectral analysis and sorting. We have demonstrated that the system is robust, hard to clog with impurities in the sample, and that the selected cells are reliably separated from the rest with minimal risk of contamination from unwanted cells.

We analyzed algal cells of *Trachydiscus minutus* according to the degree of unsaturation of their cellular lipids. We were able to analyze and sort about 12 cells per minute with high efficiency with respect to the desired chemical content, when the proportion of the selected cells was low. However, the overall efficiency of the sorting system is still only about 90 cells per hour, due to problems with steadiness of the cell delivery, and with stable and efficient recognition, trapping, and dragging of the objects, which are relatively large in terms of optical trapping. We are currently optimizing the system in these respects. The Raman-tweezers vertical

microfluidic sorting system is currently in the state of development. We want to develop a highly automated system capable of working continually for several hours without human intervention. We think it may be possible to increase the throughput to more than ten times the current effective value, over 1000 objects per hour. We hope this system will find its use for some types of cells or even inanimate microscopic objects, such as liposomes, in which the label-free metabolic profiling or chemical sensing of multiple or complex chemical variables is desired.

5 SUMMARY

In the presented doctoral thesis, we have tested the influence of optical trapping by different laser wavelengths on the individual algal cells. We have estimated the quantum yield of the photosynthetic apparatus of *Trachydiscus minutus* suspended in a culture medium, before and after optical trapping. We used several different wavelengths of the trapping laser between 735 nm and 1064 nm, with constant duration and power of irradiation. Pulse amplitude modulation fluorescence spectroscopy has detected a significant decrease of the quantum yield after irradiation by shorter wavelengths (735 nm), while at longer wavelengths (935 nm) the decrease was negligible. This finding indicates that non-invasive optical manipulation of living cells of photosynthetic microorganisms can be performed using laser wavelength longer than 950 nm.

We have demonstrated the potential of Raman microspectroscopy for the fast and spatially resolved characterization of the composition of selected intracellular compartments in individual living algal cells. In particular, we have focused on lipid storage bodies and quantified the degree of unsaturation of algal lipids. We have exploited the characteristic Raman spectral peaks corresponding to the saturated and unsaturated carbon-carbon bonds in lipid molecules. Based on the calibration data obtained with pure fatty acids of varied degree of unsaturation, we have calculated the average ratio of unsaturated-to-saturated carbon-carbon bonds in algal lipids. We have shown that various algal species display significantly different unsaturation, which has important implications for biotechnological exploitation of the particular algae. Our spectroscopic data agree with the results obtained by mass spectrometry - gas chromatography. These findings were published [21].

We found a Raman based method to measure the β-carotene concentration, which is an important parameter for selection of the production strains for biotechnology and industry. We have calculated the relative concentrations of β-carotene in the storage lipids from the Raman spectral peak ratios. The absolute concentrations were extrapolated from the calibration based on β-carotene oil solutions. The analysis of the image of the analyzed cell allowed us to calculate the volume of algal lipid bodies in absolute units, to be used as a reference measurement. The method was published [23]. Based on the LB volume measurements, simple Raman assisted

method of LB volume estimation was developed as well, and was published separately [22].

We have devised an active cell sorter with a microfluidic system to deliver the sampled microalgae to the Raman-tweezers. We found that a vertically positioned channel is superior for sorting of algal cells with diameters around 10 μm, and that a branch from the main channel can be used as an effective sorting junction, providing minimal chances for contamination with unwanted cells. We introduce the Raman tweezers based cell-sorting system, which can sort cells automatically according to the degree of unsaturation in lipid storage bodies of individual living algal cells. The resultant instrument offers a possibility to measure chemical composition of cells and to track metabolic processes *in vivo*, in real-time and label-free. In the same time, the cells can be separated depending on the input parameters obtained from Raman spectra. In this device, the cells are sorted within the microfluidic channel using such Raman spectra recorded and processed by homemade analytical and automation software developed in LabView (National Instruments). The apparatus was successfully used for cell analysis and its sorting capability was demonstrated.

6 REFERENCES

[1] **Ashkin, A.**, **Dziedzic, J. M.**, **Bjorkholm, J. E.**, **Chu, S.** Observation of a single-beam gradient force optical trap for dielectric particles. *Opt. Lett.*, 1986. volume 11, pp. 288–290.

[2] **Cižmár, T.**, **Dávila Romero, L. C.**, **Dholakia, K.**, **Andrews, D. L.** Multiple optical trapping and binding: New routes to self-assembly. *J. Phys. B: At. Mol. Opt. Phys.*, 2010. volume 43, pp. 102001.

[3] **Spalding, G.**, **Courtial, J.**, **Di Leonardo, R.** *chapter "Holographic optical trapping" in: Structured light and its applications: An introduction to phase-structured beams and nanoscale optical forces.* Elsevier Academic Press, 2008.

[4] **Dholakia, K.**, **MacDonald, M. P.**, **Zemánek, P.**, **Čižmár, T.** Cellular and colloidal separation using optical forces. *Met. in Cell Biol.*, 2007. volume 82, pp. 467–495.

[5] **Jonáš, A.**, **Zemánek, P.** Light at work: The use of optical forces for particle manipulation, sorting, and analysis. *Electrophoresis*, 2008. volume 29, pp. 4813–4851.

[6] **Petrov, D. V.** Raman spectroscopy of optically trapped particles. *J. Opt. A: Pure Appl. Opt.*, 2007. volume 9, pp. 139–156.

[7] **Rösch, P.**, **Harz, M.**, **Schmitt, M.**, **Peschke, K.-D.**, **Ronneberger, O.**, **Burkhardt, H.**, **Motzkus, H.-W.**, **Lankers, M.**, **Hofer, S.**, **Thiele, H.**, **Popp, J.** Chemotaxonomic identification of single bacteria by micro-Raman spectroscopy: Application to clean-room-relevant biological contaminations. *Appl. Environ. Microbiol.*, 2005. volume 71, pp. 1626–1637.

[8] **Mobili, P.**, **Londero, A.**, **De Antoni, G.**, **Gómez-Zavaglia, A.**, **Araujo-Andrade, C.**, **Ávila Donoso, H.**, **Ivanov-Tzonchev, R.**, **Moreno, I.**, **Frausto-Reyes, C.** Multivariate analysis of Raman spectra applied to microbiology: Discrimination of microorganisms at the species level. *Rev. Mexic. de Fisica*, 2010. volume 56, pp. 378–385.

[9] **Shih, C. J.**, **Smith, E. A.** Determination of glucose and ethanol after enzymatic hydrolysis and fermentation of biomass using Raman spectroscopy. *Anal. Chim. Acta*, 2009. volume 653, pp. 200–206.

[10] **Šerý, M.**, **Pilát, Z.**, **Jonáš, A.**, **Ježek, J.**, **Jákl, P.**, **Zemánek, P.**, **Samek, O.**, **Nedbal, L.**, **Trtílek, M.** Active sorting switch for biological objects. *SPIE Proc.*, 2010. volume 7762, pp. 776210 1–7.

[11] **Eriksson, E.**, **Scrimgeour, J.**, **Graneli, A.**, **Ramser, K.**, **Wellander, R.**, **Enger, J.**, **Hanstorp, D.**, **Goksor, M.** Optical manipulation and microfluidics for studies of single cell dynamics. *J. Opt. A: Pure Appl. Opt.*, 2007. volume 9, pp. 113–121.

[12] **Campbell-Platt, G.** Fermented foods - a world perspective. *Food Research International*, 1994. volume 27, pp. 253–257.

[13] **Mashego, M. R.**, **Rumbold, K.**, **Mey, M. D.**, **Vandamme, E.**, **Soetaert, W.**, **Heijnen, J. J.** Microbial metabolomics: past, present and future methodologies. *Biotechnol. Lett.*, 2007. volume 29, pp. 1–16.

[14] **Okonko, O.**, **Olabode, O. P.**, **Okeleji, O. S.** The role of biotechnology in the socio-economic advancement and national development: An Overview. *African J. of Biotechnol.*, 2006. volume 5, pp. 2354–2366.

[15] **Vincent, W. F.**, **Neale, P.**, **Richerson, P.** Photoinhibition: Algal responses to bright light during diel stratification and mixing in a tropical alpine lake. *J. Phycol.*, 1984. volume 20, pp. 201–211.

[16] **Barros, T.**, **Kühlbrandt, W.** Crystallisation, structure and function of plant light-harvesting Complex II. *Biochim. Biophys. Acta*, 2009. volume 1787, pp. 753–772.

[17] **Hideg, E.**, **Schreiber, U.** Parallel assessment of ROS formation and photosynthesis in leaves by fluorescence imaging. *Photosynth. Res.*, 2007. volume 92, pp. 103–108.

[18] **Ashkin, A.**, **Dziedzic, J.**, **Yamane, T.** Optical trapping and manipulation of single cells using infrared laser beams. *Nature*, 1987. volume 330, pp. 769–771.

[19] **Govindjee**. *Chlorophyll a fluorescence: A signature of photosynthesis, Series: Advances in Photosynthesis and Respiration*, volume 19. Springer Verlag, Dordrecht, 2004.

[20] **Maxwell, K.**, **Johnson, G. N.** Chlorophyll fluorescence - a practical guide. *J. Exp. Botany*, 2000. volume 51, pp. 659–668.

[21] **Samek, O.**, **Jonáš, A.**, **Pilát, Z.**, **Zemánek, P.**, **Nedbal, L.**, **Tříska, J.**, **Kotas, P.**, **Trtílek, M.** Raman microspectroscopy of individual algal cells: sensing

unsaturation of storage lipids *in vivo*. *Sensors*, 2010. volume 10, pp. 8635–8651.

[22] **Pilát, Z.**, **Bernatová, S.**, **Ježek, J.**, **Šerý, M.**, **Samek, O.**, **Zemánek, P.**, **Nedbal, L.**, **Trtílek, M.** Raman microspectroscopy of algal lipid bodies: beta-carotene as a volume sensor. *SPIE Proc.*, 2011. volume 8306, pp. 83060L:1–7.

[23] **Pilát, Z.**, **Bernatová, S.**, **Ježek, J.**, **Šerý, M.**, **Samek, O.**, **Zemánek, P.**, **Nedbal, L.**, **Trtílek, M.** Raman microspectroscopy of algal lipid bodies: beta-carotene quantification. *J. Appl. Phycol.*, 2012. volume 24, pp. 541–546.

[24] **Samek, O.**, **Pilát, Z.**, **Jonáš, A.**, **Zemánek, P.**, **Šerý, M.**, **Ježek, J.**, **Bernatová, S.**, **Nedbal, L.**, **Trtílek, M.** Characterization of microorganisms using Raman tweezers. *SPIE Proc.*, 2011. volume 8097, pp. 80970F–80970F–7.

[25] **Küpper, H.**, **Šetlík, I.**, **Trtílek, M.**, **Nedbal, L.** A microscope for two-dimensional measurements of *in vivo* chlorophyll fluorescence kinetics using pulsed measuring radiation, continuous actinic radiation, and saturating flashes. *Photosynthetica*, 2000. volume 38, pp. 553–570.

[26] **Sukenik, A.**, **Beardall, J.**, **Kromkamp, J. C.**, **Kopecký, J.**, **Masojídek, J.**, **van Bergeijk, S.**, **Gabai, S.**, **Shaham, E.**, **Yamshon, A.** Photosynthetic performance of outdoor Nannochloropsis mass cultures under a wide range of environmental conditions. *Aquat. Microb. Ecol.*, 2009. volume 56, pp. 309–322.

[27] **Schenk, P. M.**, **Thomas-Hall, S. R.**, **Stephens, E.**, **Marx, U. C.**, **Mussgnug, J. H.**, **Posten, C.**, **Kruse, O.**, **Hankamer, B.** Second Generation Biofuels: High-Efficiency Microalgae for Biodiesel Production. *BioEnergy Research*, 2008. volume 1, pp. 20–43.

[28] **Gouveia, L.**, **Marques, A.**, **da Silva, T.**, **Reis, A.** Neochloris oleabundans UTEX1185: a suitable renewable lipid source for biofuel production. *J. Ind. Microbiol. Biotechnol.*, 2009. volume 36, pp. 821–826.

[29] **Gouveia, L.**, **Oliveira, A.** Microalgae as a raw material for biofuels production. *J. Ind. Microbiol. Biotechnol.*, 2009. volume 36, pp. 269–274.

[30] **Bailey, G. F.**, **Horvat, R. J.** Raman Spectroscopic Analysis of the cis/trans Composition of Edible Vegetable Oils. *J. Am. Oil Chem. Soc.*, 1972. volume 49, pp. 494–498.

[31] **Sadeghi-Jorabchi, H.**, **Hendra, P.**, **Wilson, R.**, **Belton, P.** Determination of the total unsaturation in oils and fats by Fourier transform Raman spectroscopy. *J. Am. Oil Chem. Soc.*, 1990. volume 67, pp. 483–486.

[32] **Ozaki, Y.**, **Cho, R.**, **Ikegaya, K.**, **Muraishi, S.**, **Kawauchi, K.** Potential of near-infrared Fourier transform Raman spectroscopy in food analysis. *Appl. Spectrosc.*, 1992. volume 46, pp. 1503–1507.

[33] **Xia, Y.**, **Whitesides, G. M.** Soft lithography. *An. Rev. Mat. Sci.*, 1998. volume 28, pp. 153–184.

7 SHRNUTÍ

Předložená dizertační práce se zabývá kombinací optických mikromanipulací s mikrospektroskopickými metodami. Využili jsme laserovou pinzetu pro transport a třídění živých mikroorganismů, například jednobuněčných řas, či kvasinek. Ramanovskou spektroskopií jsme analyzovali chemické složení jednotlivých buněk a tyto informace jsme využili k automatické selekci buněk s vybranými vlastnostmi. Zkombinovali jsme pulsní amplitudově modulovanou fluorescenční mikrospektroskopii, optické mikromanipulace a jiné techniky ke zmapování stresové odpovědi opticky zachycených buněk při různých časech působení, vlnových délkách a intenzitách chytacího laseru. Vyrobili jsme různé typy mikrofluidních čipů a zkonstruovali jsme Ramanovu pinzetu pro třídění mikro-objektů, především živých buněk, v mikrofluidním prostředí.

8 ŽIVOTOPIS

Jméno: Zdeněk Pilát, Mgr.
Datum a místo narození: 13.7.1979, Praha, Česká Republika.
2000 – Gymnázium Jižní Město v Praze zakončeno maturitou s vyznamenáním z biologie, chemie, anglického a českého jazyka.
2000 – 2003 – Česká Zemědělská Univerzita v Praze, tři roky studia dokončené ve studijním programu "rostlinolékařství".
2003 – přestup do čtvrtého ročníku na Katedru Fyziologie Rostlin PřF UK v Praze.
2005 – státní zkoušky, diplomová práce na téma "Identifikace proteinového komplexu Arp2/3 v rostlinných buňkách." (Promotor Prof. Zdeněk Opatrný, opat@natur.cuni.cz) Magisterský titul obdržen v září 2005 na PřF UK.
2006 – 2009 – doktorské studium v Belgii na Universiteit Antwerpen, Department of Plant Physiology and Morphology (FYMO), téma „Enhancer trap T-DNA insertion lines for study of root cell elongation processes", (promotor Prof. Jean-Pierre Verbelen, Jean-Pierre.Verbelen@ua.ac.be) nedokončeno.
2009-současnost – doktorské studium na VUT v Brně, vědecká práce v rámci ÚPT AVČR

9 PŘEHLED PUBLIKAČNÍ ČINNOSTI

9.1 IMPAKTOVANÉ ČLÁNKY

1) PILÁT, Z., BERNATOVÁ, S., JEŽEK, J., ŠERÝ, M., SAMEK, O., ZEMÁNEK, P., NEDBAL, L., TRTÍLEK, M. Raman microspectroscopy of algal lipid bodies: beta-carotene quantification. *Journal of Applied Phycology*, 2012, vol. 24, pp. 541-546.
2) PILÁT, Z., JEŽEK, J., ŠERÝ, M., TRTÍLEK, M., NEDBAL, L., ZEMÁNEK, P. Optical trapping of microalgae at 735-1064 nm: Photodamage assessment. *Journal of Photochemistry and Photobiology B: Biology*, 2013, vol. 121, pp. 27-31

3) SAMEK, O., JONÁŠ, A., PILÁT, Z., ZEMÁNEK, P., NEDBAL, L., TŘÍSKA, J., KOTAS, P., TRTÍLEK, M. Raman microspectroscopy of individual algal cells: sensing unsaturation of storage lipids *in vivo*. *Sensors*, 2010, vol. 10, pp. 8635-8651.
4) SAMEK, O., ZEMÁNEK, P., BERNATOVÁ, S., PILÁT, Z., TELLE, H. H. Following lipids in the food chain: determination of the iodine value using Raman microspectroscopy. *Spectroscopy Europe*, 2012, vol. 24, pp. 18-21.
5) POŘÍZKA, P., PROCHÁZKA, D., PILÁT, Z., KRAJCAROVÁ, L., KAISER, J., MALINA, R., NOVOTNÝ, J., ZEMÁNEK, P., JEŽEK, J., ŠERÝ, M., BERNATOVÁ, S., KRZYŽÁNEK, V., DOBRANSKÁ, K., NOVOTNÝ, K., TRTÍLEK, M., SAMEK, O. Application of laser-induced breakdown spectroscopy to the analysis of algal biomass for industrial biotechnology. *Spectrochimica Acta Part B: Atomic Spectroscopy*, 2012, vol. 74-75, pp. 169-176.
6) BERNATOVÁ, S., SAMEK, O., PILÁT, Z., ŠERÝ, M., JEŽEK, J., JÁKL, P., ŠILER, M., KRZYŽÁNEK, V., ZEMÁNEK, P., HOLÁ, V., DVOŘÁČKOVÁ, M., RŮŽIČKA, F. Following the mechanisms of bacteriostatic versus bactericidal action using Raman spectroscopy. *Molecules*, 2013, vol. 18, pp. 13188-13199.
7) AAS, M., JONÁŠ, A., KIRAZ, A., BRZOBOHATÝ, O., JEŽEK, J., PILÁT, Z., ZEMÁNEK, P. Spectral tuning of lasing emission from optofluidic droplet microlasers using optical stretching. *Optics Express*, 2013, vol. 21, pp. 21381-21394.

9.2 SBORNÍKY

1) PILÁT, Z., BERNATOVÁ, S., JEŽEK, J., ŠERÝ, M., SAMEK, O., ZEMÁNEK, P., NEDBAL, L., TRTÍLEK, M. Raman microspectroscopy of algal lipid bodies: beta-carotene as a volume sensor. *Proceedings of SPIE* vol. 8306, pp. 83060L:1-7, 2011, Photonics, Devices, and Systems V, Praha (CZ), 24.8.-26.8. 2011.
2) SAMEK, O., PILÁT, Z., JONÁŠ, A., ZEMÁNEK, P., NEDBAL, L., TŘÍSKA, J., KOTAS, P., TRTÍLEK, M. Raman spectroscopy for the characterization of algal cells. *Proceedings of SPIE* vol. 7746, pp. 77460X:1-7, 2010, 17th Slovak-Czech-Polish Optical Conference on Wave and Quantum Aspects of Contemporary Optics, Liptovsky Jan (SK), 6.9. 2010.
3) ŠERÝ, M., PILÁT, Z., JONÁŠ, A., JEŽEK, J., JÁKL, P., ZEMÁNEK, P., SAMEK, O., NEDBAL, L., TRTÍLEK, M. Active sorting switch for biological objects. *Proceedings of SPIE* vol. 7762, pp. 776210:1-7, 2010, Optical Trapping and Optical Micromanipulation VII, San Diego (CA, USA), 1.8. 2010.
4) SAMEK, O., PILÁT, Z., JONÁŠ, A., ZEMÁNEK, P., ŠERÝ, M., JEŽEK, J., BERNATOVÁ, S., NEDBAL, L., TRTÍLEK, M. Raman microspectroscopy based sensor of algal lipid unsaturation. *Proceedings of SPIE* vol. 8073, pp. 80730O:1-6, 2011, Optical Sensors 2011 and Photonic Crystal Fibers V, Praha (CZ), 18.4.-20.4. 2011.
5) SAMEK, O., PILÁT, Z., JONÁŠ, A., ZEMÁNEK, P., ŠERÝ, M., JEŽEK, J., BERNATOVÁ, S., NEDBAL, L., TRTÍLEK, M. Characterization of

microorganisms using Raman tweezers. *Proceedings of SPIE* vol. 8097, pp. 80970F:1-7, 2011, Optical Trapping and Optical Micromanipulation VIII, San Diego (CA, USA), 21.8.-25.8. 2011.

6) JEŽEK, J., PILÁT, Z., ŠERÝ, M., KAŇKA, J., SAMEK, O., BERNATOVÁ, S., ZEMÁNEK, P. Microfluidic systems for optical sorting. *Proceedings of SPIE* vol. 8697, pp. 86970W, 2012, 18th Czech-Polish-Slovak Optical Conference on Wave and Quantum Aspects of Contemporary Optics, Ostravice (CZ), 3.9-7.9. 2012.
7) BERNATOVÁ, S., SAMEK, O., PILÁT, Z., ŠERÝ, M., JEŽEK, J., KRZYŽÁNEK, V., ZEMÁNEK, P., RŮŽICKA, F. Raman spectroscopy for bacterial identification and characterization. *Proceedings of SPIE* vol. 8697, pp. 86970Y, 2012, 18th Czech-Polish-Slovak Optical Conference on Wave and Quantum Aspects of Contemporary Optics, Ostravice (CZ), 3.9.-7.9. 2012.
8) AAS, M., JONÁŠ, A., KIRAZ, A., BRZOBOHATÝ, O., JEŽEK, J., PILÁT, Z., ZEMÁNEK, P. Tunable optofluidic microlasers based on optically stretched emulsion droplets. *Proceedings of SPIE*, vol. 8810, pp. 88101Y, 2013, Optical Trapping and Optical Micromanipulation X (Eds. K. Dholakia, G.C. Spalding), 2013.

9.3 ORÁLNÍ PREZENTACE

1) PILÁT, Z., JONÁŠ, A., SAMEK, O., JEŽEK, J., ŠERÝ, M., ZEMÁNEK, P. Optical microspectroscopy and micromanipulations for live-cell analysis and sorting in microfluidic systems. EOS meeting, Paříž, Francie, 26.10. 2010.
2) PILÁT, Z., JONÁŠ, A., SAMEK, O., JEŽEK, J., ŠERÝ, M., ZEMÁNEK, P., NOVÁK, P., NEDBAL, L. Optical microspectroscopy and micromanipulations for live-cell analysis and sorting in microfluidic systems. OTA meeting, Monterey, CA, USA, 4.4. 2011.
3) PILÁT, Z., JONÁŠ, A., SAMEK, O., JEŽEK, J., ŠERÝ, M., BERNATOVÁ, S., ZEMÁNEK, P., NOVÁK, P., NEDBAL, L. Optical microspectroscopy and micromanipulations for live-cell analysis and sorting in microfluidic systems. SPIE Photonics Prague, Praha, Česká Republika, 24.9. 2011.
4) PILÁT, Z., JEŽEK, J., ŠERÝ, M., TRTÍLEK, M., NEDBAL, L., ZEMÁNEK, P. Optické chytání jednobuněčných řas laserem s λ=735-1064 nm: hodnocení optického poškození. Konference Laser 52, Třešť, Česká Republika, 31.10. 2012.
5) PILÁT, Z., JEŽEK, J., ŠERÝ, M., BERNATOVÁ, S., KAŇKA, J., SAMEK, O., ZEMÁNEK, P. Optical trapping, diagnostics and sorting of unicellular organisms. Optical Trapping Applications (OTA) Hawaii Waikoloa Marriott Beach Resort and Spa, Waikoloa Beach, HI, USA, 10.4. 2013.
6) PILÁT, Z., JEŽEK, J., KAŇKA, J., ZEMÁNEK, P. Analysis and sorting of photoautotrophic organisms by Raman tweezers in microfluidic environment. COST meeting, University of Münster, Münster, Německo, 28.10. 2013.
7) PILÁT, Z., JEŽEK, J., KAŇKA, J., ZEMÁNEK, P. Raman tweezers in microfluidic systems for analysis and sorting of living cells. SPIE Photonics West, Moscone Center San Francisco, San Francisco, CA, USA, 1.2. 2014.

8) PILÁT, Z., JEŽEK, J., KAŇKA, J., ZEMÁNEK, P. Raman tweezers in microfluidic system for analysis and sorting of living cells. COST meeting, FOCAS Institute, Dublin, Irsko, 23.4. 2014.
9) PILÁT, Z. Analysis and sorting of photoautotrophic organisms by Raman tweezers in microfluidic environment. International Photonics Research Conference, Castle Hotel Třešť, Třešť, Česká Republika, 18.6. 2014.

9.4 POSTERY

1) PILÁT, Z., JONÁŠ, A., SAMEK, O., JEŽEK, J., ŠERÝ, M., ZEMÁNEK, P., NEDBAL, L. Spectroscopy and optical trapping of oil-rich algal cells in microfluidic systems for *in vivo* analysis and sorting. 52nd Symposium of the Society for Histochemistry, Praha, Česká Republika, 2010.
2) PILÁT, Z., JONÁŠ, A., SAMEK, O., JEŽEK, J., ŠERÝ, M., ZEMÁNEK, P., NEDBAL, L. Spectroscopy and optical trapping of oil-rich algal cells in microfluidic systems for *in vivo* analysis and sorting. COST summer school, Visegrad, Maďarsko, 2010.
3) BERNATOVÁ, S., PILÁT, Z., SAMEK, O., ŠERÝ, M., JEŽEK, J., ZEMÁNEK, P. Raman spectroscopy of optically trapped objects. Letní škola IUVSTA, Devět Skal, Česká Republika, 2011.
4) PILÁT, Z., JONÁŠ, A., SAMEK, O., BERNATOVÁ, S., JEŽEK, J., ŠERÝ, M., ZEMÁNEK, P., NEDBAL, L. Raman spectroscopy and optical trapping of oil-rich algal cells in microfluidic systems for *in vivo* analysis and sorting. ISAP 11 meeting, Halifax, Kanada, 2011.
5) PILÁT, Z., KAŇKA, J., JEŽEK, J., ZEMÁNEK, P. Raman tweezers for identification and sorting of biological objects. NOMA2013, Cetraro, Itálie, 2013.
6) PILÁT, Z., JEŽEK, J., KAŇKA, J., ZEMÁNEK, P. Raman tweezers in vertical microfluidic system for automated analysis and sorting of living cells. EMBL Conference Microfluidics 2014, EMBL, Heidelberg, Německo, 2014.
7) PILÁT, Z., JEŽEK, J., KAŇKA, J., ZEMÁNEK, P. Raman tweezers in vertical microfluidic system for automated analysis and sorting of living cells. ICORS 2014, Jena, Německo, 2014.

9.5 ZVANÉ PŘEDNÁŠKY

1) PILÁT, Z., JONÁŠ, A., SAMEK, O., JEŽEK, J., ŠERÝ, M., BERNATOVÁ, S., ZEMÁNEK, P., NOVÁK, P., NEDBAL, L. Optical microspectroscopy and micromanipulations for live-cell analysis and sorting in microfluidic systems. Ústav Přístrojové Techniky, Brno, Česká Republika, 2012. (Přednáška v rámci semináře pro zaměstnance ÚPT.)
2) PILÁT, Z. Group of optical micromanipulation techniques OMITEC. Koc University, Istanbul, Turecko, 2013. (Přednáška v rámci semináře pro studenty katedry fyziky.)

3) PILÁT, Z. Optical trapping and spectroscopic analysis of anisotropic and complex systems. University of Calabria, Cosenza, Itálie, 2013. (Přednáška v rámci semináře pro studenty katedry fyziky.)

9.6 ZAHRANIČNÍ STÁŽE

1) Research group of Professor Alper Kiraz, Department of Physics, Koc University, Istanbul, Turecko, 11.9. - 25.9. 2012.
2) Research group of Professor Alper Kiraz, Department of Physics, Koc University, Istanbul, Turecko, 2.9. - 22.9. 2013.
3) Research group of Professor Gabriella Ciparrone, Centre of Excellence for the Study of Innovative Functional Materials, University of Calabria, Cosenza, Itálie, 19.5. - 31.5. 2013. (Short term scientific mission, COST STSM.)

9.7 MEZINÁRODNÍ KONFERENCE (BEZ VLASTNÍHO PŘÍSPĚVKU)

1) Cytokinematics 2009, Univerzita Hradec Králové, Hradec Králové, Česká Republika, 9.12. 2009.
2) Microdroplets in action symposium, University of Cambridge, Cambridge, Velká Británie, 26.7. 2013.
3) FOTONIK 2013, Koc University, Istanbul, Turecko, 6.9. 2013.

9.8 UŽITNÉ VZORY

Užitný vzor č. PUV 2013-27879, Způsob třídění živých buněk fotoautotrofních mikroorganismů a zařízení pro provádění tohoto způsobu (odbočení z PV 2013-319), zapsán do rejstříku užitných vzorů pod číslem 25864, platný do 29.4. 2017.

9.9 PATENTY

Podána patentová přihláška PV 2013-319, Způsob třídění živých buněk fotoautotrofních mikroorganismů a zařízení pro provádění tohoto způsobu.

9.10 OCENĚNÍ

SPIE Student Award at the PHOTONICS PRAGUE 2011 Conference